Zoomorphology (2026) 145:8
https://doi.org/10.1007/s00435-025-00765-9

RESEARCH

Comparative analysis of locomotory organs and tracheal system in *Halarachne halichoeri*: implications for marine parasite habits

Anika Preuss[1] · Thomas van de Kamp[2,3] · Marcus Zuber[2] · Elias Hamann[2] · Lukas Brunkert[1] · Insa Herzog[4] · Kristina Lehnert[4] · Stanislav N. Gorb[1]

Received: 18 September 2025 / Revised: 1 December 2025 / Accepted: 6 December 2025

Abstract
The nasal mite *Halarachne halichoeri* thrives in a unique niche: the respiratory tracts of deep-diving seals, where it faces high hydrostatic pressures, hypoxia, and osmotic stress. Using synchrotron X-ray microtomography, 3D reconstruction, scanning electron microscopy, and confocal laser scanning microscopy, we reveal the mite's adaptations to these extreme conditions. Its specialized attachment system, comprising two claws and a dynamic pad (arolium), enables secure anchorage to the soft mucosal surfaces. When anchoring to rough surfaces, the arolium actively folds inward with the help of a sclerite-tendon mechanism, allowing the claws to firmly embed into and interlock with the substrate. In contrast, on smooth surfaces, leg and claw angles are actively adjusted by tendons to retract the claws proximally, enabling the unfolded and extended arolium to contact and adhere to the substrate. The mite's leg musculature is strongly developed, with powerful flexors and depressors ensuring stable attachment, while protractors and levators facilitate movement. The respiratory system features a highly reduced tracheal volume (only 0.04% of body volume) suggesting a predominant reliance on cuticular respiration. Thickened, taenidia-reinforced tracheae provide mechanical stability against collapse during the intense pressure changes encountered during host dives. These findings highlight the exceptional morphological and physiological strategies enabling *H. halichoeri* to survive in extreme environments.

Keywords Respiratory mite · Marine mammals · Pinnipedia · Musculature · Attachment mechanism · Tracheal system

Introduction

Arthropods are the most successful animal phylum, comprising over 80% of all described species (Roth and Brown 1976; Leggett et al. 2024; Sollai et al. 2024). Their remarkable diversification in size, shape, color, and ecological adaptations has allowed them to colonize a wide variety of habitats (Umbers et al. 2014; Aria 2022; Zabeati 2023). The Chelicerata represent a significant subphylum of Arthropoda, encompassing arachnids and their closest relatives. Presently, over 116,000 extant species have been documented, with spiders (order Araneae) and mites (subclass Acari, comprising Acariformes and Parasitiformes) constituting the majority of the recorded species (Dunlop 2019). Despite their widespread distribution, only a limited number of Chelicerata are found in marine environments (Roth and Brown 1976; Shultz 2001; Leggett et al. 2024). Among these rare occurrences is the family Halarachnidae (Arachnida, Mesostigmata), with Mesostigmata being one of the largest groups of Parasitiformes, while Halarachnidae

✉ Anika Preuss
apreuss@zoologie.uni-kiel.de

[1] Department of Functional Morphology and Biomechanics Zoological Institute, Kiel University, Am Botanischen Garten 1-9, 24118 Kiel, Germany

[2] Institute for Photon Science and Synchrotron Radiation (IPS), Karlsruhe Institute of Technology, Hermann-von-Helmholtz-Platz 1, 76344 Eggenstein-Leopoldshafen, Germany

[3] Laboratory for Applications of Synchrotron Radiation (LAS), Karlsruhe Institute of Technology (KIT), Kaiserstr.12, 76131 Karlsruhe, Germany

[4] Institute for Terrestrial and Aquatic Wildlife Research, University of Veterinary Medicine Hannover, Büsum, Germany

Published online: 09 January 2026

itself represents only a small family uniquely adapted to aquatic habitats (Furman and Dailey 1980; Alonso-Farré et al. 2012).

A distinctive feature of the genus *Halarachne* is its obligate endoparasitic lifestyle within the respiratory tract of seals (Pinnipedia) (Pesapane et al. 2021). While most mites (Acari) are free-living or act as ectoparasites on terrestrial vertebrates (Reckendorf et al. 2019), *Halarachne* evolved in close association with seal ancestors during the Oligocene (29 to 23 million years ago), coinciding with the hosts' return to the sea (Berta et al. 2015; Davis 2019b; Reckendorf et al. 2019). During this land-to-sea transition, the parasites encountered challenges, such as increased hydrostatic pressure, hypoxia, extreme temperatures, and salinity-induced osmotic stress, all of which likely drove significant behavioral and physiological adaptations (Leggett et al. 2024).

These nasal mites reside on the mucosal surface of the host's respiratory system, feeding primarily on mucus and other secretions (Alonso-Farré et al. 2012). Their life cycle comprises a hexapod larva, an adult, and two transient stages, the proto- and deutonymph, with only the hexapod larva being active enough to relocate within and between hosts. In contrast, the adults remain largely inactive, securing themselves to the nasal mucosa with their tarsal claws (Furman and Smith 1973; Geraci and St. Aubin 1987). In adult *H. halichoeri*, the opisthosoma extends into the air-filled nasal lumen, whereas the prosoma, including the stigmata, lies embedded within the mucus layer covering the nasal epithelium (Pugh 1996; Reckendorf et al. 2019). This spatial positioning exposes different body regions to different microenvironments, which may impose distinct morphological demands.

One notable representative of the genus is *Halarachne halichoeri* Allman, 1847 (Acari; Halarachnidae), which primarily infests harbor seals (*Phoca vitulina*) and grey seals (*Halichoerus grypus*). These marine predators forage extensively in the open ocean (Davis 2019a) undertaking dives that can exceed 300–600 m in depth and last 20–35 min, with surfacing speeds around 10–18 km/h (Kolb 1982; Williams and Kooyman 1985; Thompson et al. 1991; Frost et al. 2001; Gjertz et al. 2001; Hastings et al. 2004; Eguchi and Harvey 2006; Gallon et al. 2007; Hall and Russell 2018; Rosing-Asvid et al. 2020). Consequently, during such dives the mite is exposed to rapid pressure changes, reaching pressures of approximately 60 $kg \cdot cm^{-2}$ (5883.96 kPa; ~ 58 atm) at 600 m depth (Leonardi et al. 2020).

The extreme conditions of the host's diving behavior present unique challenges for the mite. Maintaining a secure grip on the soft nasal mucosa is critical; any loss of adhesion would be fatal, as the mite depends on the nasal mucus for nutrition and the adult stage is minimally active in its locomotory behavior (Furman and Smith 1973; Geraci and St. Aubin 1987; Alonso-Farré et al. 2012). Thus, one of the most important adaptations for a parasitic lifestyle includes specialized attachment organs (Fain 1994). In mites, the diversity of such structures is strongly influenced by their habitat. Typically, claws serve to secure the organism's attachment to rough surfaces, as evidenced by studies on ectoparasitic mites that often feature two claws (Helle and Sabelis 1985; Evans 1992; Pfingstl et al. 2020; Pfingstl 2023; Winand et al. 2023; Filippov et al. 2024). In addition, soft adhesive pads can complement claw function by increasing friction on smooth, rough, soft, or hard surfaces (Helle and Sabelis 1985; Beutel and Gorb 2001; Gorb and Beutel 2001; Pfingstl 2023), and pads with similar function may be present in *H. halichoeri* (Evans 1992). Nonetheless, the precise function and mechanism of these attachment organs – potentially specialized for the soft nasal mucosa and mucus – remain insufficiently understood (Pfingstl 2023).

The respiratory system of *H. halichoeri* must be adapted to withstand significant pressure changes, as calculations indicate compression of the tracheae under high pressure (Pugh 1996). Earlier investigations suggest that these mites possess a low-volume respiratory system with low oxygen demands and tracheae reinforced by taenidia, which are chitinous windings used to prevent tracheal cuticles from collapse under pressure (Pugh 1996). However, these studies did not address the material properties of the tracheae or determine their actual volume, leaving the respiratory mechanisms largely unexplored.

The aim of this study is threefold: (i) to elucidate the morphology of the attachment and locomotion systems as well as the structure and volume of the tracheal system *of H. halichoeri* using synchrotron X-ray microtomography and 3D reconstruction, (ii) to analyze the material composition and structure of the tracheae via scanning electron microscopy (SEM) and confocal laser scanning microscopy (CLSM), and (iii) to compare the musculature and tracheal volume with those of other arthropods from diverse habitats, in order to identify potential adaptations to the challenging marine environment. This research not only advances our understanding of mite parasite adaptations to extreme marine habitats, but also may inspire novel robotic attachment devices (Winand et al. 2022).

Materials and methods

Animals

From April to November 2022, respiratory mites *(H. halichoeri*; Acari; Halarachnidae) (Fig. 1A, B) were collected from deceased or critically ill harbor seals (*P. vitulina*) recovered

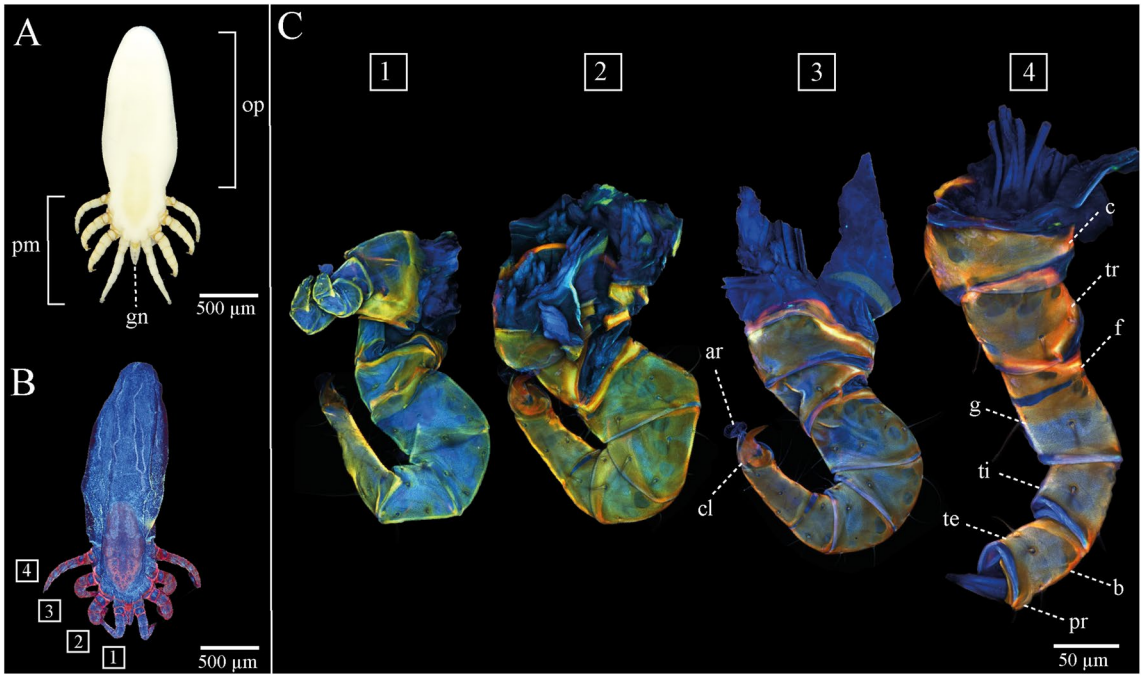

Fig. 1 *Halarachne halichoeri* and its leg morphology. **A** Light microscopic image of the general habitus from dorsal view depicting opisthosoma, prosoma and gnathosoma. **B** CLSM image from dorsal view. **C** CLSM image of all four legs numbered from anterior to posterior (see B). An enlarged CLSM image of the arolium can be found in the Supplementary Material S1. Abbreviations: arolium (ar), basitarsus (b), coxa (c), claw (cl), femur (f), gnathosoma (gn), opisthosoma (op), genu (g), pretarsus (pr), prosoma (pm), telotarsus (te), tibia (ti), trochanter (tr)

along the Baltic and North Sea shores of Schleswig-Holstein. Mite specimens were obtained during comprehensive post mortem examinations conducted as part of the Schleswig-Holstein stranding network's health monitoring program for marine mammals (Siebert et al. 2007; Herzog et al. 2024a, b; Herzog, Siebert and Lehnert 2024). For morphological studies, the gathered samples were stored in a 70% ethanol solution. There was no need for ethical review and approval for this research because all the host animals were either found deceased, died of natural causes, or were euthanized for welfare reasons, and none were killed specifically for this study. The authors did not participate in the euthanasia of the hosts, as this was carried out by certified seal rangers for reasons unrelated to the research. We have adhered to all applicable ethical guidelines concerning the use of animals.

Scanning electron microscopy (SEM)

Female adult respiratory mites ($n=3$) underwent a dehydration process involving a series of increasing alcohol concentrations (from 70 to 100%), followed by critical point drying in an automated Leica EM CPD300 system (Leica, Wetzlar, Germany). Subsequently, a Leica Bal-TEC SCD500 vacuum sputter coater was employed to apply a 10 nm gold-palladium coating to the specimens. SEM images were obtained from both sides of the samples using a Hitachi TM3000 tabletop SEM (Hitachi Ltd., Tokyo, Japan) operating at 15 kV acceleration voltage, with the aid of a rotatable sample holder (Pohl 2010). The resulting images were processed using Adobe Photoshop CS6 (Adobe Photoshop CS, San José, USA) and Affinity Photo 1.10.6 (Serif Ltd, Nottingham, UK) solely for cropping and for global adjustments of brightness and contrast.

Confocal laser scanning microscopy (CLSM)

To conduct CLSM analysis, fixed respiratory mites were immersed in glycerine (≥99.5%) and covered with a high precision cover slip (thickness = 0.170 mm ± 0.005 mm, refractive index = 1.52550 ± 0.00015, Carl Zeiss Microscopy GmbH, Jena, Germany) before scanning. The samples' autofluorescence was examined using a Zeiss LSM700 CLSM connected to an upright Zeiss Axio Imager microscope (Carl Zeiss Microscopy GmbH, Jena, Germany). The examination employed four solid-state lasers (wavelengths 405 nm, 488 nm, 555 nm, 639 nm) with corresponding emission filters (BP420–480, LP490, LP560, LP640 nm). Following the technique described by Michels and Gorb (2012), less sclerotized cuticle, potentially resilin-rich, was identified using 405 nm excitation and 420–480 nm emission filter. Areas of higher sclerotization were detected using 488 nm and 555

nm laser excitations with filters transmitting emission light above 490 nm and 560 nm respectively. Extended autofluorescence was recorded using 639 nm laser excitation with a 640 nm long-path emission filter. Image projections were processed using ZEN 2008 software (www.zeiss.de/mikroskopie) and Adobe Photoshop CS6 (Adobe Photoshop CS, San José, USA) for qualitative, but not quantitative, analysis of cuticle composition (Andersen 1979; Vincent 2002; Michels and Gorb 2012; Büsse and Gorb 2018; Josten et al. 2022). In the autofluorescence images, specific colors indicate material properties as follows: reddish autofluorescence signifies highly sclerotized cuticle, with more intense red hues indicating greater degrees of sclerotization. Greenish autofluorescence suggests relatively resilient cuticle with high chitin content, while bluish autofluorescence indicates softer, less-sclerotized cuticle areas, often containing resilin.

Synchrotron X-ray microtomography and 3D reconstruction

We used the IMAGE beamline (Cecilia et al. 2025) at KIT Light Source's Imaging Cluster to examine *H. halichoeri* specimens ($n=2$). A superconducting wiggler produced the beam, which was filtered through 2 mm pyrolytic graphite and then monochromatized at 18 keV using a Double Multilayer Monochromator (DMM). The imaging apparatus included a swift indirect detector system, consisting of a scintillator, visible light optics, a white beam microscope (Optique Peter, Lentilly, France) (Douissard et al. 2012), and a 12-bit pco.dimax high-speed camera (Excelitas PCO GmbH, Kelheim, Germany) of 2016 × 2016 pixel resolution (11 µm each). A 5x magnification yielded an effective pixel size of 2.44 µm for 3D reconstruction of the entire mite and its tracheal system, while a 10x magnification provided a pixel size of 1.22 µm for leg musculature. Scans comprised 200 dark field images, 200 flat field images, and 3000 equiangularly distributed radiographic projections over 180° at 50 fps. The concert control system (Vogelgesang et al. 2016) automated data acquisition. The UFO framework (Vogelgesang et al. 2012) managed data processing, including dark and flat field correction and phase retrieval. The Tofu software (Faragó et al. 2022) performed the final tomogram reconstruction, generating phase and absorption contrast datasets, which were then combined and converted to 8-bit volumes.

We used Amira 6.2.0 (Thermo Fisher Scientific, Waltham, US) for data segmentation and tracheal volume calculations, while we utilized Blender 3.4 (Blender Foundation, Amsterdam, Netherlands) for visualization and rendering purposes.

Results

General morphology of the body of *H. halichoeri*

The body of the nasal mite *H. halichoeri* is composed of three sections: the gnathosoma, the prosoma (fore body), and the opisthosoma (abdomen), with the latter two forming the idiosoma. The opisthosoma is relatively larger, measuring approximately 2 mm, compared to the prosoma, which measures 0.8 mm (Fig. 1). The body exhibits a prominent blue autofluorescence, indicative of a low degree of sclerotization and a flexible cuticle. Only females were examined in this study, as males were very rarely found in host material and no sexual dimorphism or male-specific modifications have been reported for this species to date (Shields et al. 2024).

The prosoma bears four pairs of legs, which vary in length but not in the number of segments (Fig. 1). Each leg comprises eight segments: coxa (c), trochanter (tr), femur (f), genu (g), tibia (ti), basitarsus (b), telotarsus (te), and pretarsus (pr). The distal segments form the tripartite tarsus, arranged from proximal to distal. It is noticeable that the reddish autofluorescence is primarily restricted to the dorsal side of the legs, in each case to the joint regions of the individual leg segments, so that these appear more sclerotized than the remaining leg regions (Fig. 1C).

The pretarsus is equipped with two claws and a pad known as the arolium, which is situated dorsally between the claws (Fig. 1C). In mites, the pretarsus forms the distal part of the tarsus (an ambulacral complex attached to the telotarsus) and serves as the articulating base for both claws and the arolium, rather than consisting of these elements. In the CLSM projection, the claws exhibit a pronounced reddish autofluorescence, indicating significant sclerotization, whereas the arolia display a bluish autofluorescence, suggesting they are likely softer and more flexible (Fig. 1C).

Leg musculature of *H. halichoeri*

Due to the bilateral symmetry of the body, the following descriptions and analyses refer exclusively to the right half of the body of an adult female nasal mite. The muscle nomenclature used here is based on Gray et al. (1997) and consists of the components (i) leg segment, (ii) muscle origin, (iii) muscle insertion, and (iv) function (Fig. 2).

Muscles can be categorized based on their functions into flexors (fl.; leg segment bending), extensors (e; leg segment stretching), depressors (d; pulls the leg segment down), levators (l; lifts the leg segment up), protractors (p; moves the leg segment forward), and retractors (r; moves the leg segment backward). When muscle bundles share the same muscle insertion or origin within a single leg segment,

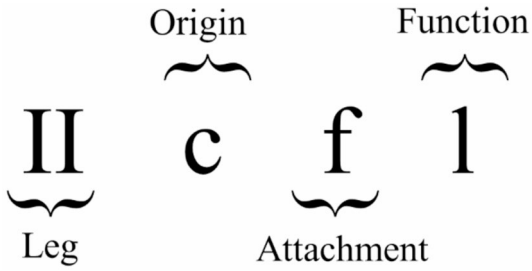

Fig. 2 Naming of the leg muscles for *H. halichoeri* according to Gray et al. (1997). The numbering of the legs in Roman numerals begins anteriorly. This is followed by the muscle origin and insertion and finally the function is named. The corresponding abbreviations can be found in Table 1. In this example, the muscle described is located in the second leg (II), starts in the coxa (c), attaches to the femur (f) and is a levator (l)

Table 1 List of abbreviations for the names of the leg muscles of *H. halichoeri* according to Gray et al. (1985)

Leg		Origin and attachment		Function	
I	1st leg	fu	furca	fl	flexor
II	2nd leg	ds	dorsalia	e	extensor
III	3rd leg	c	coxa	d	depressor
VI	4th leg	tr	trochanter	l	levator
		f	femur	p	protractor
		g	genu	r	retractor
		ti	tibia		
		b	basitarsus		
		te	telotarsus		
		pr	pretarsus		

dorsalia, or furca, and exhibit a similar trajectory, they are collectively identified as a single muscle. The leg musculature of the nasal mite comprises two categories: extrinsic muscles, with origin and insertion located entirely within the leg, and intrinsic muscles, which originate in the body (furca or prosomal body wall) and attach to the leg (Table 1).

According to Mitchell (1962), the muscle origins of the intrinsic musculature on the body wall in the prosoma are referred to as dorsalia for descriptive purposes. Dorsalia 1 and 2 are situated dorsally above the coxa of the first and second legs on the body wall. Dorsalia 3 is located dorsally and posteriorly over the coxa of the third leg, resulting in a total of three origins on the body wall in the prosoma (Fig. 3).

The furca (fu) is symmetrical and lies with its median plane in the median plane of the mite. In addition, it is centrally located between the dorsal and ventral cuticle of the idiosoma and extends from the transverse section at the anterior base of the coxa of the 2nd leg to the transverse section at the anterior base of the coxa of the 4th leg. The cuticular structures are described according to Aibekova et al. (2022) and the anterior arms of the furca are significantly longer than the posterior arms. In addition, the furca has a furca sternum on the ventral side between the furca arms (Fig. 3). The mesostigmatan furca is interpreted as homologous to the endosternite of other arachnids. According to Firstman (1973), the endosternite represents a tendon-like internal support derived from the perineural vascular membrane rather than a sclerotised exoskeletal element, suggesting

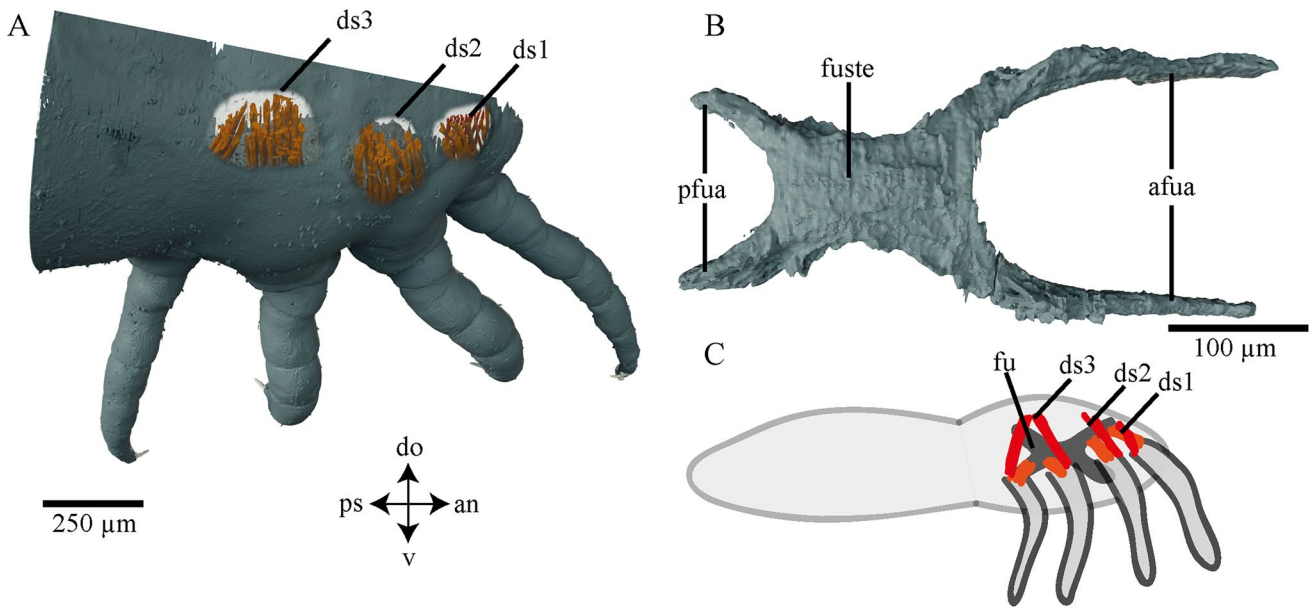

Fig. 3 Attachment sites of intrinsic musculature of *H. halichoeri*. **A** Lateral view at dorsalia (ds1, ds2, ds3). **B** Dorsal view at the furca including furca sternum and furca arms. **C** Schematic drawing of an adult mite from lateral view including intrinsic muscles connected to the furca (orange) and to the body cuticle (red). Abbreviations: anterior (an), anterior furca arm (afua), dorsal (do), dorsalia 1, 2 & 3 (ds1, ds2 & ds3), furca (fu), furca sternum (fuste), posterior (ps), posterior furca arm (pfua), ventral (v)

that the furca corresponds topologically and developmentally to this structure.

The intrinsic musculature appears to be comparable in all the legs. Notable differences are observed in the first and fourth legs, where the Idscd and IVfucr2 muscles are additionally present. Consequently, each leg comprises six or seven intrinsic muscles that contribute to the leg control and locomotion (Table 2).

In the extrinsic leg muscles, there are more differences between the legs, which can be seen in Table 3; Fig. 4, and the following text:

I-/II-/III-/IVtibfl, **gbfl**, **gtifl**, **ftifl**, **fgfl and trffl** - The muscles have two separate muscle origins in the anterior and posterior region of their respective leg segment, which converge and attach to the base of the respective segment.

II-/IIIfgp - This muscle is only present in legs 2 and 3.

II-/III-/IVtrfl1 - The muscle IIItrfl1 or IVtrfl1, respectively, has two separate muscle origins in the anterior and ventral area of the trochanter, which converge and attach to the anterior and dorsal base of the femur. The muscle is not present in the first leg. Itrfl1 only has a muscle origin in the ventral area of the trochanter.

I-/IItrfl2 - The muscle is only present in legs 1 and 2.

Overall, the extrinsic musculature of the legs is very similar in structure and there are only a few differences between the legs. The number of muscles is 15 in the first and fourth leg, 17 in the second and 16 in the third leg.

Morphology of the arolium of *H. halichoeri*

Two claws and an arolium are attached to the pretarsus of all legs, whereby the arolium lies median to the claws and overhangs them. The arolium appears blue in the CLSM maximum intensity projection, which indicates a soft, flexible structure, whereas the claws appear red and thus more sclerotized. The claws are controlled ventrally by a tendon that is moved via depressors and attached to the claw membrane connecting both claws. If tension is applied to the ventral tendon, both claws are pulled and thus brought closer to the ventral side of the pretarsus. The dorsal tendon is connected to a sclerite, which runs distally into the arolium and splits into three strands before attaching to the wall of the arolium from the inside. When tension is applied to the dorsal tendon, the sclerite is pulled proximally, causing the arolium to fold inward. This movement simultaneously lifts the claws into a more vertically oriented position. As a result, the claw tips become more exposed and can penetrate or interlock more efficiently with irregularities of a rough substrate, while the arolium no longer interferes with claw contact (Fig. 5).

Tracheal system

The nasal mite *H. halichoeri* has two spiracles (one on each side) with which its tracheal system is connected to the outside world dorsally above the coxa of the fourth leg. The

Table 2 Origin, attachment and function of the intrinsic leg muscles of an adult female *H. halichoeri*

Muscle	Muscle origin leg I	Muscle origin leg II	Muscle origin leg III	Muscle origin leg IV	Muscle attachment	Function
I-/II-/III-/IV fucr1	Anterolateral, ventral area of the right anterior furca arm	Ventral, posterolateral area of the right anterior furca arm	Ventral and anterior region of the right posterior furca arm	Ventral and posterior region of the right posterior furca arm	Posterior base of the coxa	Posterior retractor coxa
I-/II-/III-/IV fucd1	Ventromedial and posterior region of the right anterior furca arm	Medial area of the furca sternum	Medial area of the furca sternum and posterior to IIIfucd2	Ventromedial region of the right posterior furca arm	Ventral base of the coxa	Ventral depressor coxa
I-/II-/III-/IV fucd2	Ventromedial area of the right anterior furca arm	Ventromedial area from the right anterior furca arm lateral to IIfucp	Anterolateral area of the furca sternum and anterior to IIIfucd1	Posterior area of the furca sternum	Ventral base of the coxa and between fucd1 and fucp	Ventral and anterior depressor coxa
I-/II-/III-/IV fucp	Ventromedial and anterior region of the right anterior furca arm	Ventromedial area from the right anterior furca arm and medial to IIfucd2	Anteromedial region of the furca sternum	Ventral and anterior region of the right posterior furca arm	Ventral and anterior base of the coxa	Protractor coxa
I-/II-/III-/IV futrp	Ventral, anterolateral area of the right anterior furca arm	Ventrolateral area of the right anterior furca arm	Lateral area of the furca sternum	Ventrolateral area of the right posterior furca arm	Anterior base of trochanter and proximal to ctrp	Proximal protractor trochanter
I-/II-/III-/IV dscl	Dorsalia 1 and lateral to Idscd	Dorsalia 2	Dorsalia 3 and anterior to IVdscl	Dorsalia 3 and posterior to IIIdscl	Dorsal base of the coxa	Levator coxa
IVfucr2	-	-	-	Ventrolateral and posterior region of the right anterior furca arm	Dorsal and posterior base of the coxa	Dorsal retractor coxa
Idscd	Dorsalia 1 and medial to dscl	-	-	-	Anterior base of the coxa	Anterior depressor coxa

Table 3 Origin, attachment and function of the extrinsic leg muscles of an adult female *H. halichoeri*

Muscle	Origin	Attachment	Function
I-/II-/III-/IV bprl	Dorsal area of the basitarsus and distal to bprd	Dorsal tendon, which attaches to the sclerite inside the arolium	Levator; pulls the arolium in proximal direction
I-/II-/III-/IV bprd	Dorsal area of basitarsus and proximal to bprl	Ventral tendon, which attaches in the ventral area at the claw membrane in the pretarsus	Depressor of the claws
I-/II-/III-/IV tiprd	Dorsal area of the tibia and distal to tibfl	Ventral tendon, which attaches in the ventral area of the claw membrane in the pretarsus	Depressor of the claws
I-/II-/III-/IV tibfl	Dorsal area of the tibia and proximal to tiprd	Ventral base of basitarsus and distal to gbfl	Distal flexor basitarsus
I-/II-/III-/IV gbfl	Dorsal area of the genu and distal to gtifl	Ventral base of basitarsus and proximal to tibfl	Proximal flexor basitarsus
I-/II-/III-/IV gtifl	Dorsal area of the genu and proximal to gbf	Ventral base of the tibia and distal to ftifl	Distal flexor tibia
I-/II-/III-/IV ftifl	Dorsal area of femur and distal to fgfl	Ventral base of the tibia and proximal to gtifl	Proximal flexor tibia
I-/II-/III-/IV fgfl	Dorsal area of femur and proximal to ftifl	Ventrolateral base of the genu	Flexor genu
I-/II-/III-/IV fge	Ventral and proximal area of the femur	Ventral base of the genu and proximal to fgp	Extensor genu
II-/III fgp	Posterior and proximal area of the femur	Ventral base of the genu and distal to fgfl	Protractor genu
I-/II-/III-/IV trfl1	Ventral area of the trochanter and distal to trfl1	Ventral base of the femur	Flexor femur
II-/III-/IV trfl1	Ventral area of the trochanter and proximal to trfl1	Anterior and dorsal base of the femur	Anterior levator femur
I-/IItrfl2	Ventral and posterior area of the trochanter	Ventral and posterior base of the femur	Ventral levator femur
I-/II-/III-/IV cfl	Ventral area of the coxa and distal to ctrl	Dorsal base of the femur	Dorsal levator femur
I-/II-/III-/IV ctrp	Posterior area of the coxa and proximal to ctrr	Anterior base of trochanter and distal to futrp	Distal protractor trochanter
I-/II-/III-/IV ctrl	Ventral area of the coxa and proximal to cfl	Posterior base of the trochanter	Levator trochanter
I-/II-/III-/IV ctrr	Posterior area of the coxa and distal to ctrp	Ventral and posterior base of the trochanter	Retractor trochanter

two spiracles are connected to each other via a transverse connection, which runs ventrally between the coxa of the third and fourth leg. The tracheal system can be divided into the prosomal (pm) and opisthosomal (op) areas (Fig. 1). These two passages differ in structure. The prosomal region begins with three tracheae that branch off from the spiracle and divide dichotomously. The resulting tracheal branches lie anteriorly and medially in the prosoma. One trachea lies ventral to the other two and the cross-connecting duct departs from it. Three tracheae branch off from the spiracle in the opisthosomal region, which run laterally and almost parallel in the opisthosoma. Tracheae with smaller diameters generally branch off from them through a non-dichotomous division. The trachea, which lies ventral to the other two, has a special feature. It divides dichotomously once in the prosoma and later twice in the opisthosoma (Fig. 6).

The cuticle of the nasal mite shows a uniform blue autofluorescence with a presumably very low degree of sclerotization. The tracheae, on the other hand, show a yellowish autofluorescence, which indicates a higher degree of sclerotization, and they even glow clearly through the presumably thin transparent cuticula in the fluorescence projection (Fig. 6D). Within the tracheae, groove-like, regular structures can be recognized, which are taenidia (~ 1 µm wide and 0.5 µm protruding/high per taenidia) contributing to the mechanical reinforcement of trachea (Fig. 6C).

The nasal mite has a total body volume of 1.4229 µl, of which the tracheal system accounts for 0.0006 µl. This results in a ratio of tracheal volume to body volume of approximately 0.04%.

Discussion

General morphology of the body and legs

Halarachne halichoeri is characterized by a cylindrical, prolate-spheroid ("cigar-like") body shape and a dorsal shield, with the posterior section of this shield being wider and more rounded than the anterior section. In contrast, the opisthosoma of the elephant seal mite *H. miroungae* is sac-like in shape, whereas that of walrus nasal mite *Orthohalarachne attenuata* is elongated and tapers from anterior to posterior direction (Shields et al. 2024). These differences currently appear to be primarily taxonomic characters, as no direct functional role of body shape in attachment has been demonstrated. However, variation in opisthosomal form may relate to the available volume within the host's nasal cavity or the thickness of the mucus layer, since the opisthosoma is the body region most consistently exposed to the airspace for cuticular respiration (Pugh 1996; Reckendorf et

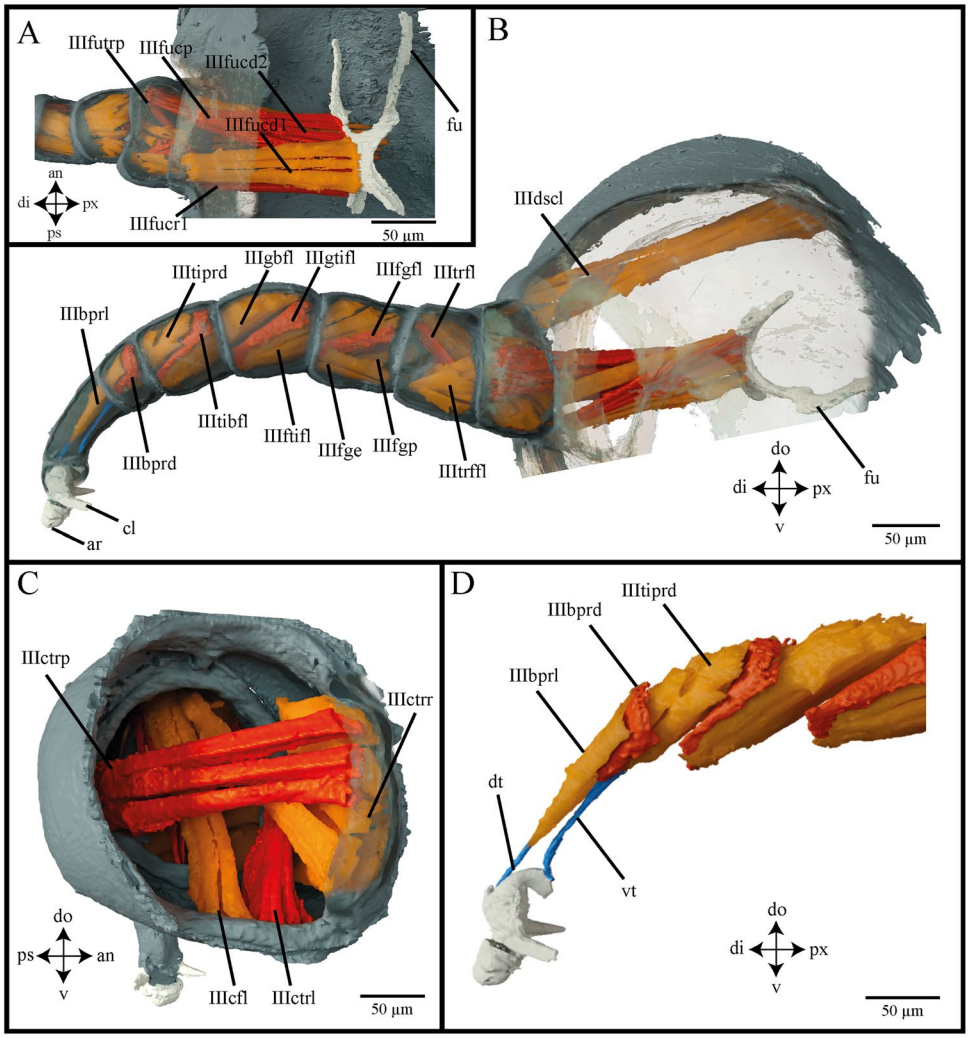

Fig. 4 Intrinsic and extrinsic leg musculature of *H. halichoeri*. **A** Dorsal view of intrinsic musculature. **B** Lateral view of intrinsic and extrinsic musculature with transparent cuticle. **C** Median view of intrinsic and extrinsic musculature. **D** Lateral view of extrinsic musculature without cuticle. Abbreviations: anterior (an), arolium (ar), cl (claw), dorsal (do), distal (di), dorsal tendon (dt), furca (fu), posterior (ps), proximal (px), ventral (v), ventral tendon (vt). Reconstructions of all other legs can be found in the Supplementary Material S2

al. 2019). Any such relationship remains hypothetical and warrants future investigation.

In representatives of the Acariformes, such as *Unionicola aegyptiaca*, *U. fossulata*, and *Najadicola ingens*, the coxa is integrated within the body, rendering it immobile (Mitchell 1955, 1962; Ramadan et al. 2019). Conversely, in *H. halichoeri*, a representative of the Parasitiformes, the coxa is freely movable (Coons and Rothschild 2008). In contrast to the mentioned representatives of the Acariformes, the origins of the intrinsic leg musculature in *H. halichoeri* are located at the furca and the dorsalia (Fig. 2). In other species, a comparable furca is absent, and thus the coxal epimers (outgrowths of the coxa) and the dorsalia serve as attachment points (Mitchell 1955, 1962; Ramadan et al. 2019). The coxal epimers are not developed in *H. halichoeri*; however, the absence of coxa stiffening and the muscle insertions on the furca situated in the median plane facilitate more flexible movement of the leg segments, if compared to the Acariformes (Coons and Rothschild 2008). Despite the general biomechanical expectation that reduced podomere mobility increases structural stiffness and thus resistance during attachment, the freely movable coxa in *H. halichoeri* may be advantageous in a different way. Instead of providing passive rigidity, coxal mobility likely allows fine-scale repositioning of the legs without disengaging the claws, enabling the mite to adjust its posture while remaining anchored within the irregular and compliant mucosal landscape of the nasal cavity. In this interpretation, flexibility at the proximal joint facilitates anchorage rather than compromising it, by improving contact angle control and load distribution during attachment.

In *H. halichoeri*, leg movement is primarily facilitated by three pairs of muscular antagonists: protractors/retractors, flexors/extensors, and levators/depressors (Snodgrass 1952). All legs across all segments contain six flexors, which function to retract the legs towards the body. In the nasal mite, this likely facilitates the anchoring of claws within the soft mucosa, thereby ensuring a secure attachment. This is particularly crucial for adult respiratory mites, which exhibit a primarily sessile lifestyle within the respiratory tract of

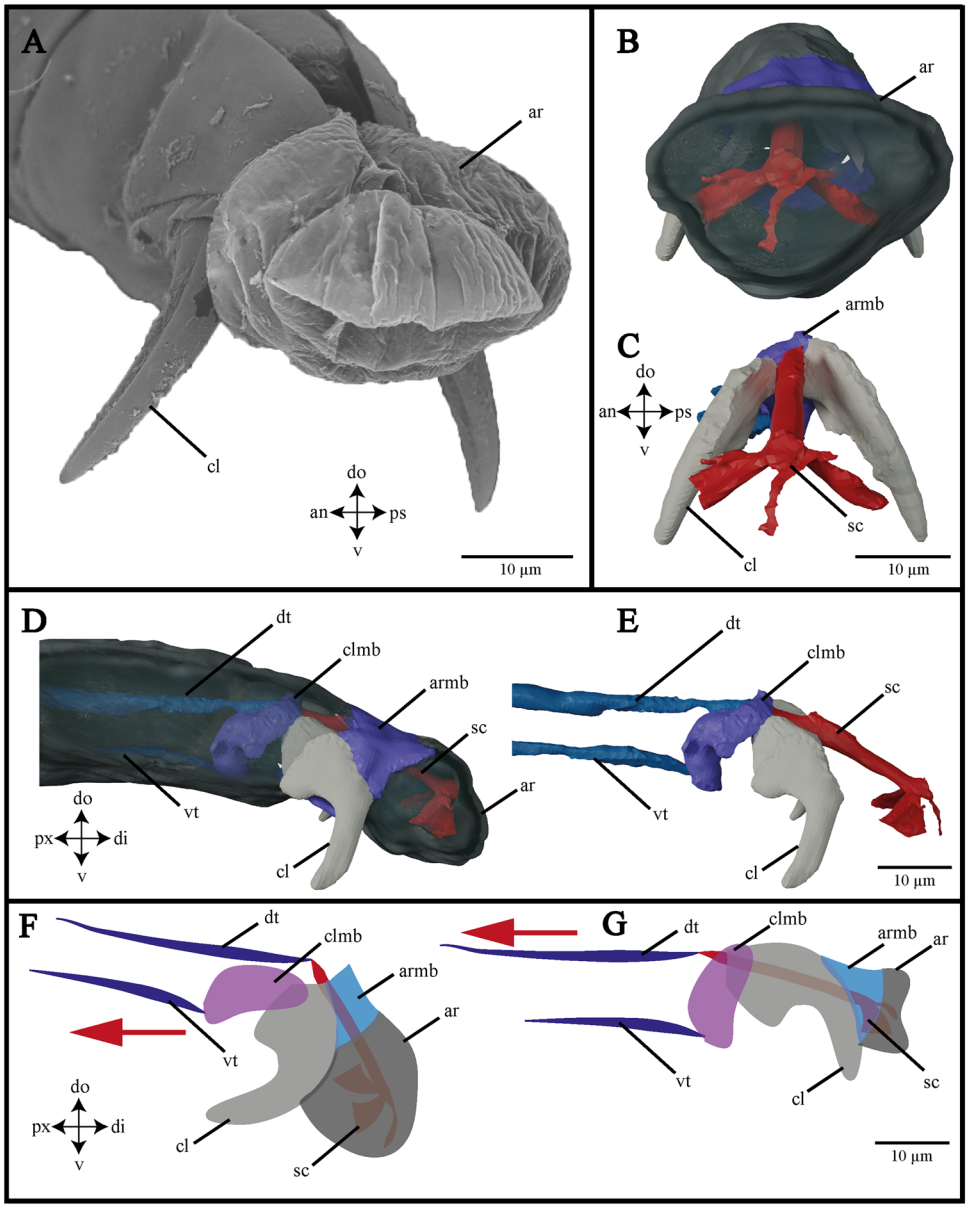

Fig. 5 Morphology of the arolium and mode of arolium attachment in *H. halichoeri*. **A** Scanning electron microscopy image of the pretarsus, extended arolium and claws. **B** 3D reconstruction of the morphology of the arolium from distal view with transparent arolium. **C** 3D reconstruction of the morphology of the arolium from distal view without arolium walls. **D** 3D reconstruction of the pretarsus including claws and arolium with transparent cuticle from lateral view. **E** 3D reconstruction of the pretarsus including claws and arolium without cuticle from lateral view. **F** Model of the claw movement when pulling the ventral tendon in the proximal direction. **G** Model of the sclerite movement when pulling the dorsal tendon in the proximal direction. Abbreviations: anterior (an), arolium (ar), arolium membrane (armb), claw (cl), claw membrane (clmb), dorsal (do), distal (di), dorsal tendon (dt), posterior (ps), proximal (px), sclerite (sc), ventral (v) ventral tendon (vt)

their hosts, necessitating a stable and secure anchorage at wet slimy surfaces (Furman and Smith 1973; Geraci and St. Aubin 1987).

In contrast, each leg possesses only a single extensor muscle dedicated to the specific extension of the leg. Additional extension of the legs, serving as a counter-movement to flexion, can occur in nasal mites through alterations in body shape and the consequent increase in hemolymph pressure within the leg (Parry and Brown 1959; Mitchell 1962). In general, it is presumed that this particular change in body shape in Acari is induced by the dorso-ventral compression of the opisthosoma (Schmelzle et al. 2015), although this aspect was not further investigated in the present study. Hydraulic leg extension, facilitated by hemolymph pressure, is a well-documented phenomenon in spiders and other large arachnids (Parry and Brown 1959; Alexander 1967; Shultz 1991). Hydraulic force transmission has even been demonstrated outside the locomotory system, for example in spider chelicerae, suggesting that pressure-mediated movement is a more widespread arachnid strategy than previously assumed (Wood and Shultz 2025). Nonetheless, exceptions exist, such as the terrestrial Southern California endemic mite *Paratarsotomus macropalpis* (Rubin et al. 2016). In this species, hydraulic leg extension is unlikely, as the viscosity of the hemocoelic fluid would impede the fluid's movement through the legs' narrow hemolymph canals at the velocities required to sustain the observed rapid stride frequencies (Sensenig and Shultz 2003; Rubin et al. 2016). Research suggests that these mites likely extend their primary leg joints by utilizing energy stored in compressed,

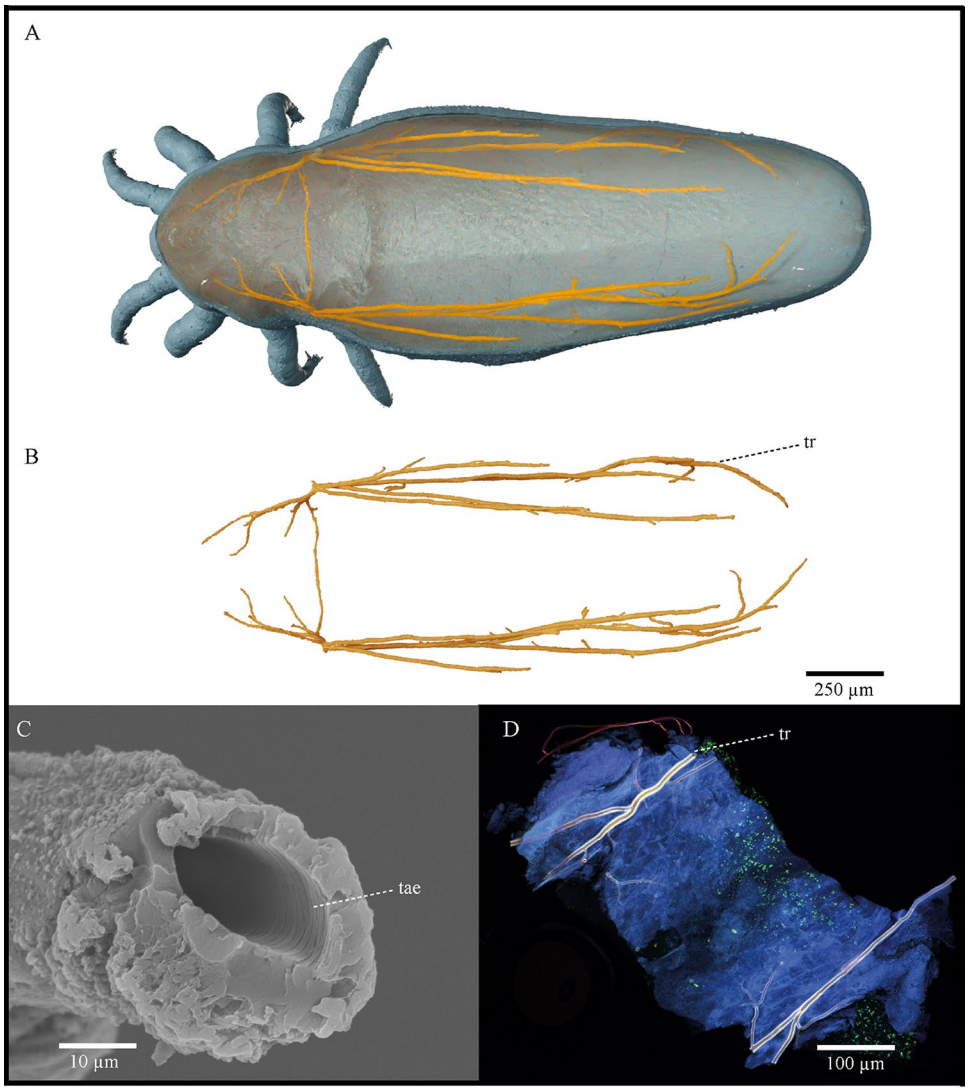

Fig. 6 Tracheal system of *H. halichoeri*. **A** Whole body from dorsal view with transparent cuticle and visible tracheal system (gold). **B** Exported tracheal system (gold). **C** Scanning electron microscopy image of a single trachea including taenidia. **D** Confocal laser scanning microscopy image of the tracheal system. Abbreviations: taenidia (tae), trachea (tr)

rather stiff but elastic sclerites (Sensenig and Shultz 2003, 2004). The lack of extensor muscles may confer the benefit of reducing leg mass and inertia, thereby diminishing the kinetic energy required to sustain high stride frequencies (Full and Tu 1990). In the respiratory mite, however, the bluish autofluorescence of the mite's cuticle suggests a high degree of flexibility, which implies that the alteration in body shape and the consequent increase in hemolymph pressure constitute the mechanism facilitating leg extension (Fig. 1).

Morphology of the arolium

Although antagonistic musculature is otherwise largely absent in the Acari, it can still be found, for example, in the claw region and in the chelicerae (Heethoff and Koerner 2007; Heethoff and Norton 2009). In *H. halichoeri* the muscles attaching to the dorsal tendon are levators (I-/II-/III-/IV bprl), which actively pull the arolium in proximal direction, resulting in an inward folding of the arolium (Fig. 5). (Preuss et al., 2025), first described this regular inward folding of the arolium of the respiratory mite, *O. attenuata* (Acari; Halarachnidae), a respiratory mite living in the respiratory tract of walruses (Fravel and Procter 2016; Pesapane et al. 2021; Rivera-Luna et al. 2023). When the mite is clinging to a rough and/or soft substrate, such as the nasal mucosa of its host, its claws are securely anchored into the fibrous substrate, while the arolium appears to be retracted inward. Conversely, when the mite walks over a smooth surface, such as the mucosa covered with the wet and slimy host mucus, claws are drawn in the proximal direction, resulting in only the arolium making contact with the substrate. Yet, Preuss et al. (Preuss et al., 2025) could not explain the mechanism behind this inward folding. Our reconstruction has facilitated the identification of a direct connection between the dorsal tendon in the pretarsus of the mite *H. halichoeri* and another tendon or sclerite extending to the distal inner wall of the arolium. Consequently, the levators exert force

on the dorsal tendon (dt), which subsequently acts on the sclerite (sc), resulting in the complete inward retraction of the arolium (ar). This action may also induce a slight dorsal movement of the claw (cl) until it is halted by the dorsal cuticle of the pretarsus (Fig. 5). The folding of the arolium upon contact with rough surfaces facilitates the engagement of the claws with the substrate. Conversely, depressor muscles (I-/II-/III-/IV bprd and I-/II-/III-/IV tiprd), which are connected to the ventral tendon (vt), move the entire pretarsus proximally to alter the angle of leg attachment, thereby allowing the extended arolium (ar) to make contact with smooth surfaces. Additionally, the claws are retracted proximally, aligning them parallel to the substrate, thus preventing interference with the arolium's contact.

These observations indicate that claws and arolium form a complementary attachment system with distinct functional roles: the claws primarily serve to anchor the mite by interlocking with the fibrous nasal mucosa of the host, whereas the arolium facilitates locomotion and stable contact on smooth, mucus-covered surfaces by increasing the effective contact area. Under such conditions, adhesion is most likely mediated by wet adhesion, including viscosity-dependent Stefan adhesion and capillary forces, as known for biological attachment systems operating on moist substrates (Nachtigall 1974; Emerson and Diehl 1980; Hanna and Barnes 1991). Importantly, this mechanism does not involve suction: neither the folding motion nor the morphology of the arolium indicates the formation of a sealed cavity or pressure differential comparable to true suction organs (Nachtigall 1974). A comparable pad-supported adhesion mode has recently been demonstrated in *O. attenuata*, where successful movement on smooth substrates required deployment of the arolium (Preuss et al., 2025). In contrast, on soft mucosal tissue, however, the claws presumably provide the primary means of attachment through mechanical interlocking, as suggested by comparable attachment strategies in other mite lineages (Heethoff and Koerner 2007; Pfingstl 2023). We therefore assume that both structures contribute to secure attachment, but that their functional importance varies with substrate properties: the claws anchor the mite on compliant mucosal surfaces, whereas the arolium enhances adhesion on smooth and wet substrates through increased contact area and fluid-mediated forces. Although adults often remain sessile, occasional locomotion within the nasal cavity is essential for repositioning and mate finding (Furman and Smith 1973; Geraci and St. Aubin 1987). In such situations, the arolium likely plays a crucial role alongside the claws by enabling controlled detachment and forward stepping, especially on smooth or mucus-coated surfaces where interlocking alone may be insufficient and inefficient.

This dynamic interplay between claws and arolium in *H. halichoeri* reflects broader principles observed in other arthropod taxa, though with notable differences in detail and control (Song et al. 2016). In many insects, such as grasshoppers (Slifer 1950), stick insects (Walther 1969), cockroaches (Arnold 1974; Frazier et al. 1999), and flies (Walker et al. 1985), the pretarsal adhesive pads are mechanically linked to the claws via a tendon. There, pad position is typically a passive consequence of claw movement (Slifer 1950; Arnold 1974; Federle et al. 2001), and the claws are typically held in position by the unguitractor plate within the insect tarsus allowing for reduced muscular efforts due to a specific interlocking mechanism (Radnikow and Bässler 1991; Bußhardt and Gorb 2014; Gorb et al. 2019). A more complex mechanism is found in Hymenoptera, where active control over arolium extension is achieved through contraction of the unguitractor muscle, hemolymph pressure, and the elasticity of the cuticle of the arolium (Snodgrass 1956; Federle et al. 2001, 2002; Frantsevich and Gorb 2002, 2004; Gladun et al. 2009). In these insects, the extension and inflation of the arolium is indirectly coupled with claw retraction: the unguitractor muscle pulls on a tendon connected to the unguitractor plate and the claws, while hemolymph pressure inflates the arolium (Federle et al. 2001, 2002). As a result, the arolium is activated through the contraction and relaxation of the claw flexor muscle: usually, the claws first retract until they reach a nearly perpendicular position relative to the tarsus, followed by the unfolding of the arolium. Detachment occurs in the reverse order. Consequently, the arolium will not unfold at all if the claws catch prematurely on a rough surface and fail to reach this perpendicular position (Snodgrass 1956; Federle 2002). For unfolding, the tendon pulled back by the unguitractor muscle allows hemolymph to inflate the soft arolium; when the tendon is released, the arolium deflates due to the recoil of its elastic cuticle (Federle et al. 2001).

In summary, the two systems achieve a similar functional outcome – substrate-specific deployment of the arolium – but through fundamentally different architectures: in *H. halichoeri*, direct tendons and a sclerite mechanically fold and unfold the arolium, whereas in Hymenoptera, an indirect coupling via the unguitractor plate combines muscle action with hydraulic inflation. This likely represents a case of convergent evolution towards effective attachment strategies under very different ecological conditions, such as mucosal surfaces in respiratory mites and varying plant surfaces in hymenopterans. Further comparative studies of internal pretarsal anatomy will be necessary to determine, whether this mechanism is unique to *H. halichoeri* and probably other Halarachnidae such as *O. attenuata* or shared among other mite taxa, whereby an expansion and retraction of adhesive pads could be observed, for example, in ticks, but without

detailed explanation of the underlying control mechanism (Voigt and Gorb 2017).

Tracheal system

The examination of the general morphology of the tracheal system, encompassing the prosomal and opisthosomal regions, the cross-connecting duct, and the various divisions of the tracheae within these areas, aligns with previous findings on the respiratory system of *H. halichoeri* (Pugh 1996), except that we were able to identify a third main tracheal stem in the opisthosoma. This observation is consistent with findings for the genus *Orthohalarachne*, which belongs to the same family Halarachnidae, as *H. halichoeri* (Finnegan 1934; Newell 1947).

The trachea exhibits a yellowish autofluorescence, indicative of a robust yet flexible cuticle. According to Pugh (1996), *H. halichoeri* possesses a notably thick intima (the non-cellular lining of the tracheal tubes) within the primary opisthosomal strains, which constitute approximately 80% of the total tracheal air space. However, the degree of sclerotization diminishes with a reduction in diameter (Fig. 6), and calculations suggest that the tracheae in the opisthosoma are also compressed with a thicker intima at a host diving depth of 30–100 m (Bostrom et al. 2008). Notably, the diving depth of grey seals typically ranges from 60 to 100 m, with recorded depths exceeding 300 m (Thompson et al. 1991) and 300 to 600 m for harbor seals (Rosing-Asvid et al. 2020). Therefore, contrary to previous findings, it can be inferred that the more stable tracheae in the opisthosoma are also subject to compression due to pressure at certain diving depths (Leonardi et al. 2020). During the diving process, the tracheae in the prosoma are compressed initially, and during the surfacing phase, the tracheae in the opisthosoma regain their original shape first, owing to the elastic intima with the taenidia (Thompson et al. 1991; Pugh 1996). Although nasal mites are usually referred to as semi-aquatic endoparasites, since they reside in the nasal cavity of their hosts (Euzet and Combes 1998; Poulin 2011), and the hosts close their nostrils during dives (Dudzinski et al. 2009), the gas in the nasopharynx of the seals is nevertheless compressed with increasing diving depth, which is consequently transferred to the nasal mites. At diving depths of ~30–100 m, the tracheae are predicted to collapse, and only the taenidia likely prevent a complete flattening of the tubes (Bostrom et al. 2008). Thus, tracheal gas transport is no longer feasible. While we were able to quantify total tracheal air volume, the resolution of the dataset does not allow measurement of terminal branch diameters and tracheoles across complete bifurcation levels. Whether the branching network of *H. halichoeri* follows Murray's law of vessel scaling therefore remains unresolved, but the progressive tapering of primary tracheal stems indicates that future high-resolution analyses may meaningfully test this.

Previous work suggested that *H. halichoeri* may rely predominantly on cuticular gas exchange, particularly through the thin opisthosomal cuticle (Pugh 1996). Our findings support this interpretation: the exceptionally small tracheal volume of *H. halichoeri* (0.04% of total body volume) indicates that oxygen uptake via the tracheal system likely plays only a minor role in adults, especially during prolonged host dives. In combination with the flexible and weakly sclerotized opisthosomal cuticle observed in our CLSM data, this strongly suggests that cuticular respiration represents the primary mode of gas exchange. The positional arrangement of body regions within the host further reinforces this conclusion: while the prosoma containing the stigmata is typically embedded in the mucus layer during attachment, the opisthosoma protrudes freely into the air-filled nasal lumen (Pugh 1996; Reckendorf et al. 2019), probably enabling cuticle respiration through this flexible and weakly sclerotized cuticle area.

Most arthropod species that have secondarily returned to the sea, which is the case for *H. halichoeri*, generally rely on aerial respiration (Raga et al. 2009; Berta et al. 2015; Vermeij 2020). In this context, "secondarily returned to the sea" refers to the evolutionary origin of the lineage, whereas the description as a semi-aquatic endoparasite reflects its current lifestyle within the air-filled nasal cavity of marine mammals. Cuticular respiration is likely sufficient to meet the basic oxygen demand of this small and largely inactive mite. To further conserve oxygen, *H. halichoeri* probably reduces its metabolic rate, which aligns with the pronounced sedentary behavior of adult individuals (Reckendorf et al. 2019). A comparable strategy is known from seal lice (Echinophthiriidae), which enter metabolic depression ("akinesis") to reduce oxygen consumption and energy expenditure (Kim 1975; Koštál 2006; Leonardi and Lazzari 2014; Leonardi et al. 2020; Preuss, Schwaha, et al., 2025).

In contrast to *H. halichoeri*, the tracheal systems of many insects occupy a substantially larger proportion of the body (~49% in *Calliphora vicina* and ~40% in *Schistocerca americana*), which can be attributed to their larger body size, higher metabolic demands, or more oxygen-dependent lifestyles (Lease et al. 2006; Harrison et al. 2010; Wasserthal et al. 2018). Even in comparably sized insects, such as the red flour beetle, *Tribolium castaneum* (Kaiser et al. 2007), or the seal louse, *Echinophthirius horridus*, the proportion of tracheal volume to body volume is about 12 times higher (Preuss, Schwaha, et al., 2025). Larger insects have to invest proportionally more in their tracheal systems than smaller insects, reflecting the well-established allometric scaling of respiratory volume with body size. Likewise, insects living in hypoxic conditions typically possess enlarged tracheal

systems compared to those in hyperoxic environments. Experimental studies indicate that chronic hypoxia can lead to substantial tracheal expansion, including increased branching and air sac volume, whereas hyperoxia causes the opposite effect. Although the magnitude of this change varies strongly among taxa and developmental stages, published examples range from moderate increases in tracheal diameter to dramatic enlargement of air sacs under hypoxic treatment, while hyperoxia repeatedly results in measurable reductions in tracheal investment (Harrison et al. 2010). Additional factors influencing tracheal volume include the presence of air sacs, particularly in flying insects, such as flies and grasshoppers (Lease et al. 2006) or book lungs in arachnids, which consist of internal chambers with numerous thin, leaf-like lamellae stacked like the pages of a book. Here, air enters through a small slit called a spiracle, and gas exchange takes place across the surface of the lamellae (Levi 1967; Küntzel et al. 2019). However, in the case of *H. halichoeri*, the lower need for a well-developed tracheal system is mitigated by its small size, lack of flight, and the probable capacity to drastically reduce its metabolic rate (Leonardi and Lazzari 2014; Leonardi et al. 2020). As a result, this mite can probably rely on the limited oxygen stored in its small tracheal network and body tissues, and cuticle respiration, allowing it to survive extended periods even under low-oxygen conditions.

Conclusion

This study provides new insights into the remarkable adaptations of *H. halichoeri* for life in the challenging environment of a seal's respiratory tract. Through a combination of advanced imaging techniques, we have uncovered how the mite's specialized attachment structures and respiratory system enable survival under extreme conditions. The pretarsal apparatus, featuring two claws and an arolium, shows a finely tuned functional duality: when anchoring to rough surfaces, the arolium folds inward, allowing the claws to embed securely; on smooth surfaces, the claws are retracted proximally by tendon action, adjusting the leg angle to deploy the extended arolium for optimal adhesion. While claws alone likely maintain static anchorage, the arolium may become particularly important during locomotion and mate search, enabling controlled detachment and stepwise progression across smooth or mucus-coated surfaces. This dynamic mechanism demonstrates a sophisticated level of biomechanical control rarely described but possibly commonly present in mites.

The mite's leg musculature is equally specialized, with powerful flexors and depressors designed to maximize attachment force, supporting a sessile lifestyle in the host's mucus-rich environment. Additionally, the highly reduced tracheal system, occupying only 0.04% of body volume, and the presence of thickened, taenidia-reinforced tracheae point towards a strong reliance on cuticular respiration and a minimized oxygen demand during host dives. These findings not only deepen our understanding of parasite adaptations to extreme aquatic environments, but also offer promising models for biologically inspired applications, such as underwater adhesion and flexible respiratory technologies, although such applications remain speculative. Overall, *H. halichoeri* exemplifies the set of extraordinary evolutionary innovations necessary to secondarily adapt to one of the most inhospitable microhabitats.

Supplementary Information The online version contains supplementary material available at https://doi.org/10.1007/s00435-025-00765-9.

Acknowledgements We extend our gratitude to Dr. Thies Büscher, Dr. Helen Gorges, Fabian Bäumler, Julian Thomas, Simon Züger, and Benedikt Josten for their invaluable contributions and support throughout our study. Our thanks also go to Esther Appel and Dr. Alexander Kovalev for their technical assistance during the experimental phases of our research. We are indebted to Dr. Angelica Cecilia for her assistance during beamtime and to Dr. Tomáš Faragó for his work on tomographic reconstructions. We express our gratitude to the KIT Light Source for providing instruments at their beamlines and to the Institute for Beam Physics and Technology (IBPT) for operating the storage ring, the Karlsruhe Research Accelerator (KARA). We are deeply thankful for the financial support provided to S.N.G. and K.L. through the grant GO 995 46-1 and LE 4753/4-1 from the German Science Foundation (DFG) as part of the Special Priority Program (SPP 2332) "Physics of Parasitism". The funding organizations did not participate in the study's design, data collection and analysis, publication decisions, or manuscript preparation.

Author contributions A.P., S.N.G.—Conceptualisation; A.P.—Data curation; A.P.—Formal analysis; K.L., S.N.G.—Funding acquisition; A.P., T.V.D.K, I.H., L.B., S.N.G.—Investigation; A.P., T.V.D.K., M.Z., E.H., S.N.G.—Methodology; S.N.G—Project administration; K.L., S.N.G.—Resources; A.P., T.V.D.K.—Software; S.N.G.—Supervision; A.P., T.V.D.K., S.N.G.—Validation; A.P., L.B.—Visualisation; A.P.—Writing—original draft; T.V.D.K., L.B., M.Z., E.H., I.H., K.L., S.N.G.—Writing – review & editing.

Funding Open Access funding enabled and organized by Projekt DEAL.

Data availability The data that supporting study are available in the Supplementary Material. CT-data can be accessed via https://figshare.com/s/3363a94e47e510c593dc.

Declarations

Conflict of interest The authors declare no competing interests.

References

Aibekova L et al (2022) The skeletomuscular system of the mesosoma of *Formica Rufa* workers (Hymenoptera: Formicidae). Insect Syst Divers 6(2):1–26. https://doi.org/10.1093/isd/ixac002

Alexander AJ (1967) Problems of limb extension in the scorpion, *Opisthophthalmus latimanus* Koch. Trans R Soc S Afr 37(3):165–181. https://doi.org/10.1080/00359196709519065

Alonso-Farré JM, D'Silva JID, Gestal C (2012) Naso-pharyngeal mites *Halarachne halichoeri* (Allman, 1847) in grey seals stranded on the NW Spanish Atlantic coast. Vet Parasitol 183(3):317–322. https://doi.org/10.1016/j.vetpar.2011.08.002

Andersen SO (1979) Biochemistry of insect cuticle. Ann Rev Entomol 24(1):29–59. https://doi.org/10.1146/annurev.en.24.010179.000333

Aria C (2022) The origin and early evolution of arthropods. Biol Rev 97(5):1786–1809. https://doi.org/10.1111/brv.12864

Arnold JW (1974) Adaptive features on the tarsi of cockroaches (Insecta: Dictyoptera). Int J Insect Morphol Embryol 3(3):317–334. https://doi.org/10.1016/0020-7322(74)90026-9

Berta A, Sumich JL, Kovacs KM (2015) 'Chaper 1 - Introduction', in A. Berta, J.L. Sumich, and K.M. Kovacs (eds) *Marine Mammals: Evolutionary Biology*. 3rd edn. San Diego, California (US): Academic Press, pp. 1–14. https://doi.org/10.1016/B978-0-12-397002-2.00001-6

Beutel RG, Gorb SN (2001) Ultrastructure of attachment specializations of hexapods (Arthropoda): evolutionary patterns inferred from a revised ordinal phylogeny. J Zool Syst Evol Res 39(4):177–207. https://doi.org/10.1046/j.1439-0469.2001.00155.x

Bostrom BL, Fahlman A, Jones DR (2008) Tracheal compression delays alveolar collapse during deep diving in marine mammals. Respir Physiol Neurobiol 161(3):298–305. https://doi.org/10.1016/j.resp.2008.03.003

Büsse S, Gorb SN (2018) Material composition of the mouthpart cuticle in a damselfly larva (Insecta: Odonata) and its biomechanical significance. R Soc Open Sci 5(6):172117. https://doi.org/10.1098/rsos.172117

Bußhardt P, Gorb SN (2014) Ground reaction forces in vertically ascending beetles and corresponding activity of the claw retractor muscle on smooth and rough substrates. J Comp Physiol A Neuroethol Sens Neural Behav Physiol 200(5):385–398. https://doi.org/10.1007/s00359-014-0896-0

Cecilia A et al (2025) The IMAGE beamline at the KIT Light Source. J Synchrotron Radiat 32(4):1036–1051. https://doi.org/10.1107/s1600577525003777

Coons LB, Rothschild M (2008) 'Mites (Acari).' Encyclopedia of Entomology. Springer, Dordrecht, Netherlands, pp 2413–2441. https://doi.org/10.1007/978-1-4020-6359-6_4636

Davis RW (2019a) 'Introduction.' Marine Mammals: Adaptations for an Aquatic Life. Springer, Cham, Germany, pp 1–5. https://doi.org/10.1007/978-3-319-98280-9_1

Davis RW (2019b) 'Return to the sea: the evolution of marine mammals.' Marine Mammals: Adaptations for an Aquatic Life. Springer International Publishing, Cham, Germany, pp 7–27. https://doi.org/10.1007/978-3-319-98280-9_2

Douissard PA et al (2012) A versatile indirect detector design for hard X-ray microimaging. J Instrum. https://doi.org/10.1088/1748-0221/7/09/P09016

Dudzinski KM, Thomas JA, Gregg JD (2009) 'Communication in marine mammals.' In: Perrin WF, Würsig B, Thewissen JGM (eds) Encyclopedia of Marine Mammals, 2nd edn. Academic Press, San Diego, California (US), pp 260–269. https://doi.org/10.1016/B978-0-12-373553-9.00064-X

Dunlop JA (2019) Miniaturisation in chelicerata. Arthropod Struct Dev 48:20–34. https://doi.org/10.1016/j.asd.2018.10.002

Eguchi T, Harvey J (2006) Diving behavior of the Pacific harbor seal (*Phoca vitulina richardii*) in Monterey Bay, California. Mar Mamm Sci 21:283–295. https://doi.org/10.1111/j.1748-7692.2005.tb01228.x

Emerson SB, Diehl D (1980) Toe pad morphology and mechanisms of sticking in frogs. Biol J Linn Soc 13(3):199–216. https://doi.org/10.1111/j.1095-8312.1980.tb00082.x

Euzet L, Combes C (1998) The selection of habitats among the monogenea. Int J Parasitol 28(10):1645–1652. https://doi.org/10.1016/S0020-7519(98)00062-9

Evans GO (1992) Principles of Acarology. In: Evans GO (ed). CAB International, Wallingford, UK

Fain A (1994) Adaptation, specificity and host-parasite coevolution in mites (Acari). Int J Parasitol 24(8):1273–1283. https://doi.org/10.1016/0020-7519(94)90194-5

Faragó T et al (2022) Tofu: a fast, versatile and user-friendly image processing toolkit for computed tomography. J Synchrotron Radiat 29:916–927. https://doi.org/10.1107/S160057752200282X

Federle W (2002) An integrative study of insect adhesion: mechanics and wet adhesion of pretarsal pads in ants. Integr Comp Biol 42(6):1100–1106. https://doi.org/10.1093/icb/42.6.1100

Federle W et al (2001) Biomechanics of the movable pretarsal adhesive organ in ants and bees. Proc Natl Acad Sci U S A 98(11):6215–6220. https://doi.org/10.1073/pnas.111139298

Filippov AE et al (2024) Solid lubricant in the insect leg joints: numerical simulation of tribological properties. Adv Theory Simulations 7(7):2400348. https://doi.org/10.1002/adts.202400348

Finnegan S (1934) On a new species of mite of the family Halarachnidae from the Southern sea Lion. Discoveries Rep 8:319–328

Firstman B (1973) The relationship of the chelicerate arterial system to the evolution of the endosternite. J Arachnology 1(1):1–54. http://www.jstor.org/stable/3705296

Frantsevich L, Gorb S (2002) Arcus as a tensegrity structure in the arolium of wasps (Hymenoptera: Vespidae). Zoology 105(3):225–237. https://doi.org/10.1078/0944-2006-00067

Frantsevich L, Gorb S (2004) Structure and mechanics of the tarsal chain in the hornet, *Vespa Crabro* (Hymenoptera: Vespidae): implications on the attachment mechanism. Arthropod Struct Dev 33(1):77–89. https://doi.org/10.1016/j.asd.2003.10.003

Fravel V, Procter D (2016) Successful diagnosis and treatment of *Orthohalarachne attenuata* nasal mites utilising voluntary rhinoscopy in three Pacific Walrus (*Odobenus Rosmarus divergens*). Veterinary Record Case Rep 4(1):e000258. https://doi.org/10.1136/VETRECCR-2015-000258

Frazier SF et al (1999) Elasticity and movements of the cockroach tarsus in walking. Journal of Comparative Physiology - A Sensory, Neural, and Behavioral Physiology 185(2):157–172. https://doi.org/10.1007/s003590050374

Frost KJ, Simpkins MA, Lowry LF (2001) Diving behavior of subadult and adult harbor seals in Prince William Sound, Alaska. Mar Mamm Sci 17(4):813–834. https://doi.org/10.1111/j.1748-7692.2001.tb01300.x

Full BYRJ, Tu MS (1990) Mechanics of six-legged runners. J Exp Biol 148(1):129–146. https://doi.org/10.1242/jeb.148.1.129

Furman DP, Dailey MD (1980) The genus *Halarachne* (Acari: Halarachnidae), with the description of a new species from the Hawaiian monk seal. J Med Entomol 17(4):352–359. https://doi.org/10.1093/jmedent/17.4.352

Furman DP, Smith AW (1973) In vitro development of two species of *Orthohalarachne* (Acarina: Halarachnidae) and adaptations of the life cycle for endoparasitism in mammals. J Med Entomol 10(4):415–416. https://doi.org/10.1093/jmedent/10.4.415

Gallon SL et al (2007) How fast does a seal swim? Variations in swimming behaviour under differing foraging conditions. J Exp Biol 210(18):3285–3294. https://doi.org/10.1242/jeb.007542

Geraci JR, St. Aubin DJ (1987) Effects of parasites on marine mammals. Int J Parasitol 17(2):407–414. https://doi.org/10.1016/0020-7519(87)90116-0

Gjertz I, Lydersen C, Wiig Ø (2001) Distribution and diving of harbour seals (*Phoca vitulina*) in Svalbard. Polar Biol 24(3):209–214. https://doi.org/10.1007/s003000000197

Gladun D, Gorb SN, Frantsevich LI (2009) Alternative tasks of the insect arolium with special reference to Hymenoptera. Functional Surfaces in Biology. Springer Dordrecht, Dordrecht, Netherlands, pp 67–103. https://doi.org/10.1007/978-1-4020-6695-5_4

Gorb SN, Beutel R (2001) Evolution of locomotory attachment pads of hexapods. Naturwissenschaften 88(12):530–534. https://doi.org/10.1007/s00114-001-0274-y

Gorb SN et al (2019) The insect unguitractor plate in action: force transmission and the micro CT visualizations of inner structures. J Insect Physiol 117:103908. https://doi.org/10.1016/j.jinsphys.2019.103908

Gray PTA, Mill PJ, Dodd JM (1997) The musculature of the prothoracic legs and its innervation in *Hierodula membranacea* (Mantidea). Philos Trans R Soc Lond B Biol Sci 309(1140):479–503. https://doi.org/10.1098/rstb.1985.0094

Hall AJ, Russell DJF (2018) 'Gray seal: Halichoerus grypus.' In: Würsig B, Thewissen JGM, Kovacs KM (eds) Encyclopedia of Marine Mammals, 3rd edn. Academic Press, San Diego, California (US), pp 420–422. https://doi.org/10.1016/B978-0-12-804327-1.00139-4

Hanna G, Barnes WJP (1991) Adhesion and detachment of the toe pads of tree frogs. J Exp Biol 155(1):103–125

Harrison JF, Kaiser A, VandenBrooks JM (2010) Atmospheric oxygen level and the evolution of insect body size. Proc R Soc Lond B Biol Sci 277(1690):1937–1946. https://doi.org/10.1098/rspb.2010.0001

Hastings KK et al (2004) Regional differences in diving behavior of harbor seals in the Gulf of Alaska. Can J Zool 82(11):1755–1773. https://doi.org/10.1139/z04-145

Heethoff M, Koerner L (2007) Small but powerful: the oribatid mite *Archegozetes longisetosus* Aoki (Acari, Oribatida) produces disproportionately high forces. J Exp Biol 210(17):3036–3042. https://doi.org/10.1242/jeb.008276

Heethoff M, Norton RA (2009) Role of musculature during defecation in a particle-feeding arachnid, *Archegozetes longisetosus* (Acari, Oribatida). J Morphol 270(1):1–13. https://doi.org/10.1002/jmor.10667

Helle W, Sabelis MW (1985) Spider Mites. Their Biology, natural enemies and control, 1st edn. Elsevier, Amsterdam, Netherlands. https://doi.org/10.1111/j.1570-7458.1987.tb03606.x

Herzog I et al (2024) Heartworm and seal louse: trends in prevalence, characterisation of impact and transmission pathways in a unique parasite assembly on seals in the North and Baltic Sea. Int J Parasitol Parasites Wildl 23:100898. https://doi.org/10.1016/j.ijppaw.2023.100898

Herzog I, Siebert U, Lehnert K (2024b) High prevalence and low intensity of *Echinophthirius horridus* infection in seals revealed by high effort sampling. Sci Rep 14(1):14258. https://doi.org/10.1038/s41598-024-64890-z

Josten B, Gorb SN, Büsse S (2022) The mouthparts of the adult dragonfly *Anax imperator* (Insecta: Odonata), functional morphology and feeding kinematics. J Morphol 283(9):1163–1181. https://doi.org/10.1002/jmor.21497

Kaiser A et al (2007) Increase in tracheal investment with beetle size supports hypothesis of oxygen limitation on insect gigantism. Proc Natl Acad Sci U S A 104(32):13198–13203. https://doi.org/10.1073/pnas.0611544104

Kim KC (1975) Ecology and morphological adaptations of the sucking lice on the nothern fur seal. J Cons Int Explor Mer 169:504–515

Kolb PM (1982) A harbor seal, *Phoca vitulina richardsi*, taken from a sablefish trap. Calif Fish Game 68:123–124

Koštál V (2006) Eco-physiological phases of insect diapause. J Insect Physiol 52(2):113–127. https://doi.org/10.1016/j.jinsphys.2005.09.008

Küntzel N, Dunlop JA, Scholtz G (2019) Morphology and evolution of spider book lungs (Araneae). Arthropod Syst Phylogeny 77(2):267–284. https://doi.org/10.26049/ASP77-2-2019-05

Lease HM, Wolf BO, Harrison JF (2006) Intraspecific variation in tracheal volume in the American locust, *Schistocerca americana*, measured by a new inert gas method. J Exp Biol 209(17):3476–3483. https://doi.org/10.1242/jeb.02343

Leggett MA, Vink CJ, Nelson XJ (2024) Adaptation and survival of marine-associated spiders (Araneae). Annu Rev Entomol 69:481–501. https://doi.org/10.1146/annurev-ento-062923-102457

Leonardi MS, Lazzari CR (2014) Uncovering deep mysteries: the underwater life of an amphibious louse. J Insect Physiol 71:164–169. https://doi.org/10.1016/j.jinsphys.2014.10.016

Leonardi MS et al (2020) Under pressure: the extraordinary survival of seal lice in the deep sea. J Exp Biol 223(17):jeb226811. https://doi.org/10.1242/jeb.226811

Levi HW (1967) Adapations of respiratory systems of spiders. Evolution 21(3):571–583. https://doi.org/10.2307/2406617

Michels J, Gorb SN (2012) Detailed three-dimensional visualization of resilin in the exoskeleton of arthropods using confocal laser scanning microscopy. J Microsc 245(1):1–16. https://doi.org/10.1111/j.1365-2818.2011.03523.x

Mitchell RD (1955) Anatomy, life history, and evolution of mites parasitizing fresh-water mussels. Misc Publ Mus Zool Univ Mich 89(89):1–28

Mitchell RD (1962) The musculature of a trombiculid mite, *Blankaartia ascoscutellaris* (Walch). Ann Entomol Soc Am 55(1):106–119. https://doi.org/10.1093/aesa/55.1.106

Nachtigall W (1974) Biological mechanisms of attachment: The comparative morphology and bioengineering of organs for linkage, suction, and adhesion, 1st edn. Springer Berlin, Heidelberg, Heidelberg, Germany. https://doi.org/10.1007/978-3-642-85775-1

Newell IM (1947) Studies on the morphology and systematics of the family Halarachnidae Oudemans 1906 (Acari, Parasitoidea). Bingham, New York (US): Bingham Oceanographic Laboratory

Parry DA, Brown RHJ (1959) The hydraulic mechanism of the spider leg. J Exp Biol 36(2):423–433. https://doi.org/10.1242/jeb.36.2.423

Pesapane R et al (2021) Nasopulmonary mites (Halarachnidae) of coastal Californian pinnipeds: identity, prevalence, and molecular characterization. Int J Parasitol Parasites Wildl 16:113–119. https://doi.org/10.1016/j.ijppaw.2021.08.005

Pfingstl T (2023) Sharp claws beneath our feet–the diversity of tarsal attachment devices of oribatid mites (Acari, Chelicerata, excluding Astigmata)–a review. Int J Acarol 49(3–4):165–195. https://doi.org/10.1080/01647954.2023.2223214

Pfingstl T, Kerschbaumer M, Shimano S (2020) Get a grip-evolution of claw shape in relation to microhabitat use in intertidal arthropods (Acari, Oribatida). PeerJ 8:e8488. https://doi.org/10.7717/peerj.8488

Pohl H (2010) A scanning electron microscopy specimen holder for viewing different angles of a single specimen. Microsc Res Tech 73(12):1073–1076. https://doi.org/10.1002/jemt.20835
Poulin R (2011) Evolutionary ecology of parasites, 2nd edn. Princeton University Press, Princeton, New Jersey (US)
Preuss A, Ebmer D, Gorb EV et al (2025) Locomotion and attachment mechanisms of the respiratory mite *Orthohalarachne attenuata*. Exp Appl Acarol 95:66. https://doi.org/10.1007/s10493-025-01094-8s A, Ebmer D et al (2025) 'Locomotion and attachment mechanisms of the respiratory mite Orthohalarachne attenuata', Experimental and Applied Acarology , in pres
Preuss A, Schwaha T et al (2025) The ectoparasitic seal louse, *Echinophthirius horridus*, relies on a sealed tracheal system and spiracle closing apparatus for underwater respiration. Commun Biology 8(1):1–14. https://doi.org/10.1038/s42003-025-08285-4
Pugh PJA (1996) The respiratory system of *Halarachne halichoeri* (Halarachnidae: Gamasida: Anactinotrichida). J Zool 239(2):285–300. https://doi.org/10.1111/j.1469-7998.1996.tb05452.x
Radnikow G, Bässler U (1991) Function of a muscle whose apodeme travels through a joint moved by other muscles: why the retractor unguis muscle in stick insects is tripartite and has no antagonist. J Exp Biol 157(1):87–99. https://doi.org/10.1242/jeb.157.1.87
Raga JA (2009) 'Parasites.' In: Perrin WF, Würsig B, Thewissen JGM (eds) Encyclopedia of Marine Mammals, 2nd edn. Academic Press, London, UK, pp 821–830. https://doi.org/10.1016/B978-0-12-373553-9.00193-0
Ramadan SA, Ismail TG, Mustafa AN (2019) Studies on the cuticle and musculature of freshwater mite, *Unionicola aegyptiaca*. The Journal of Basic and Applied Zoology 80:66. https://doi.org/10.1186/s41936-019-0133-z
Reckendorf A et al (2019) There and back again – the return of the nasal mite *Halarachne halichoeri* to seals in German waters. Int J Parasitol Parasites Wildl 9:112–118. https://doi.org/10.1016/j.ijppaw.2019.04.003
Rivera-Luna H et al (2023) Non-invasive detection of *Orthohalarachne attenuata* (Banks, 1910) and *Orthohalarachne diminuata* (Doetschman, 1944) (Acari: Halarachnidae) in free-ranging synanthropic South American sea lions *Otaria flavescens* (Shaw, 1800). Int J Parasitol Parasites Wildl 21:192–200. https://doi.org/10.1016/j.ijppaw.2023.06.001
Rosing-Asvid A et al (2020) Deep diving harbor seals (*Phoca vitulina*) in South Greenland: movements, diving, haul-out and breeding activities described by telemetry. Polar Biol 43(4):359–368. https://doi.org/10.1007/s00300-020-02639-w
Roth VD, Brown VV (1976) 'Other intertidal air-breathing arthropods. ' in Cheng L. (eds) Marine insects. North-Holland Publishing Company, Amsterdam, Netherlands, pp 119–150
Rubin S et al (2016) Exceptional running and turning performance in a mite. J Exp Biol 219(5):676–685. https://doi.org/10.1242/jeb.128652
Schmelzle S, Norton RA, Heethoff M (2015) Mechanics of the ptychoid defense mechanism in ptyctima (Acari, Oribatida): one problem, two solutions. Zool Anz J Comp Zool 254:27–40. https://doi.org/10.1016/j.jcz.2014.09.002
Sensenig AT, Shultz JW (2003) Mechanics of cuticular elastic energy storage in leg joints lacking extensor muscles in arachnids. J Exp Biol 206(4):771–784. https://doi.org/10.1242/jeb.00182
Sensenig AT, Shultz JW (2004) Elastic energy storage in the pedipalpal joints of scorpions and sun-spiders (Arachnida, Scorpiones, Solifugae). J Arachnol 32(1):1–10. https://doi.org/10.1636/S02-73
Shields MM, Roth T, Pesapane R (2024) A pictorial key to the adult and larval nasal mites (Halarachnidae) of marine mammals. ZooKeys 2024(1216):101–114. https://doi.org/10.3897/zookeys.1216.135359
Shultz JW (1991) Evolution of locomotion in Arachnida: the hydraulic pressure pump of the giant whipscorpion, *Mastigoproctus giganteus* (Uropygi). J Morphol 210(1):13–31. https://doi.org/10.1002/jmor.1052100103
Shultz JW (2001) 'Chelicerata (arachnids, including spiders, mites and scorpions).' Encyclopedia of Life Sciences. John Wiley & Sons, Ltd, New York, New York (US), pp 1–5. https://doi.org/10.1038/npg.els.0001605
Siebert U et al (2007) Pathological findings in harbour seals (*Phoca vitulina*): 1996–2005. J Comp Pathol 137(1):47–58. https://doi.org/10.1016/j.jcpa.2007.04.018
Slifer EH (1950) Vulnerable areas on the surface of the tarsus and pretarsus of the grasshopper (Acrididae, Orthoptera); with special reference to the arolium. Ann Entomol Soc Amer 43(2):173–188. https://doi.org/10.1093/aesa/43.2.173
Snodgrass RE (1952) Textbook of arthropod anatomy. Cornell University Press, Ithaca, New York (US)
Snodgrass RE (1956) Anatomy of the Honey Bee. Cornell University Press, Ithaca, New York (US)
Sollai G et al (2024) Topic: arthropod biodiversity: ecological and functional aspects. Insects 15(10):766. https://doi.org/10.3390/insects15100766
Song Y et al (2016) The synergy between the insect-inspired claws and adhesive pads increases the attachment ability on various rough surfaces. Sci Rep 6:1–9. https://doi.org/10.1038/srep26219
Thompson D et al (1991) Movements, diving and foraging behaviour of grey seals (*Halichoerus grypus*). J Zool 224(2):223–232. https://doi.org/10.1111/j.1469-7998.1991.tb04801.x
Umbers KDL et al (2014) Reversible colour change in Arthropoda. Biol Rev 89(4):820–848. https://doi.org/10.1111/brv.12079
Vermeij GJ (2020) The ecology of marine colonization by terrestrial arthropods. Arthropod Struct Dev 56:100930. https://doi.org/10.1016/j.asd.2020.100930
Vincent JFV (2002) Arthropod cuticle: a natural composite shell system. Compos Part A-Appl Sci Manuf 33(10):1311–1315. https://doi.org/10.1016/S1359-835X(02)00167-7
Vogelgesang M et al (2012) 'UFO: a scalable GPU-based image processing framework for online monitoring', in *Proceedings of HPCC-ICESS.*, pp. 824–829. https://doi.org/10.1109/HPCC.2012.116
Vogelgesang M et al (2016) Real-time image-content-based beamline control for smart 4D X-ray imaging. J Synchrotron Radiat 23(5):1254–1263. https://doi.org/10.1107/S1600577516010195
Voigt D, Gorb SN (2017) Functional morphology of tarsal adhesive pads and attachment ability in ticks *Ixodes ricinus* (Arachnida, Acari, Ixodidae). J Exp Biol 220(11):1984–1996. https://doi.org/10.1242/jeb.152942
Walker G, Yulf AB, Ratcliffe J (1985) The adhesive organ of the blowfly, *Calliphora vomitoria*: a functional approach (Diptera: Calliphoridae). J Zool 205(2):297–307. https://doi.org/10.1111/j.1469-7998.1985.tb03536.x
Walther C (1969) Zum verhalten des krallenbeugersystems Bei der Stabheuschrecke *Carausius morosus* Br. Z für Vergleichende Physiologie 62(4):421–460. https://doi.org/10.1007/BF00299266
Wasserthal LT et al (2018) X-ray computed tomography study of the flight-adapted tracheal system in the blowfly *Calliphora vicina*, analysing the ventilation mechanism and flow-directing valves. J Exp Biol 221(12):jeb176024. https://doi.org/10.1242/jeb.176024
Williams TM, Kooyman GL (1985) Swimming performance and hydrodynamic characteristics of harbor seals *Phoca vitulina*. Physiol Zool 58(5):576–589. https://doi.org/10.1086/physzool.58.5.30158584
Winand J, Büscher T, Gorb SN (2022) Learning from nature: a review on biological gripping principles and their application to robotics. Soft Robotics. Bentham Science, Sharjah, United Arab Emirates, pp 21–59. https://doi.org/10.2174/9789815051728122010l
Winand J, Gorb SN, Büscher TH (2023) Gripping performance in the stick insect *Sungaya inexpectata* in dependence on the pretarsal

architecture. J Comp Physiol A 209(2):313–323. https://doi.org/10.1007/s00359-022-01570-1
Wood HM, Shultz JW (2025) The role of hydraulic pressure in spider cheliceral function. Arthropod Struct Dev 88:101475. https://doi.org/10.1016/j.asd.2025.101475
Zabeati L (2023) Arthropodology the earth's most diverse group of animals. Int J Pure Appl Zool 11(4):10–11. https://doi.org/10.35841/2320-9585-11.4.187